Research Journal of Applied Sciences, Engineering and Technology 4(22): 4685-4695,2012
ISSN: 2040-7467

Submitted: March 26, 2012 Accepted: April 17, 2012 Published: November 15, 2012

Two-Phase Cavitating Flow in Turbomachines

[1]Sandor I. Bernad, [2]Romeo Susan-Resiga and [1]Sebastian Muntean
[1]Romanian Academy-Timisoara Branch, Centre for Fundamental and Advanced Technical Research Bd. Mihai Viteazul 24, RO-300223, Timisoara, Romania
[2]Department of Hydraulic Machinery, University "Politehnica" of Timisoara, Bd. Mihai Viteazul 1, RO-300222, Timisoara, Romania

Abstract: Cavitating flows are notoriously complex because they are highly turbulent and unsteady flows involving two species (liquid/vapor) with a large density difference. These features pose a unique challenge to numerical modeling works. The study briefly reviews the methodology curently employed for industrial cavitating flow simulations using the two-phase mixture model. The two-phase mixture model is evaluated and validated using benchmark problem where experimental data are available. A 3D cavitating flow computation is performed for the GAMM Francis runner. The model is able to qualitatively predict the location and extent of the 3D cavity on the blade, but further investigation are needed to quatitatively assess the accuracy for real turbomachinery cavitating flows.

Keywords: Cavitation, francis turbine, liquid-vapour interface, vapour volume

INTRODUCTION

Cavitation is one of the major problems that hinder the hydraulic machinery performances. Once the flow velocity and blade loading are increased there are regions where the pressure drops well below the vaporization pressure of the liquid and cavitation is developed. The associated noise and vibrations, as well as cavitation erosion, have motivated a great number of theoretical and experimental studies with the aimed at elucidating both cavitation physics and its practical consequences such as errosion and vibrations (Anton, 1984). So far, the cavitation bubble dynamics in newtonian fluids and the associated phenomena are well understood. On the other hand, cavitation in hydraulic machinery is a complex, three-dimensional unsteady phenomena which has yet to be studied both theoretically and experimentally.

The ability to model cavitating flows has drawn strong interest in CFD community. It covers a wide range of applications, such as pumps, hydraulic turbines, marine propellers, hydrofoils, inducers and fuel cavitation in orifices as commonly encountered in fuel injection systems.

Fluid machinery is a common application where low pressures are routinely generated by the machine action, e.g., on blade surfaces, with a consequent possibility of cavitation. Existence of cavitation is often undesired, because it can degrade the device performance, produce undesirable noise, lead to physical damage to the device and affect the structural integrity. Details of the existence, extent and effects of cavitation can be of significant help during the design stages of fluid machinery, in order to minimize cavitation or to account for its effects and optimize the design.

Past several decades have seen considerable research on cavitation and extensive reviews are available in the literature (Anton, 1984; Li, 2000; Kueny, 1993). Different aspects of this complex phenomenon have been explored, including, e.g., cavitation bubble collapse (Wang and Brennen, 1994) and erosion damage, cavitation acoustics, cloud cavitation (Wang and Brennen, 1994; Wang *et al*., 2001) and rotating cavitation (Avellan *et al*., 1990; Avellan *et al*., 1993).

Based on the assumption that the flow is inviscid, various numerical methods have been thus far proposed to simulate cavitating fows; the conformal mapping method, the singularity method and the panel method. The flow around hydrofoil (Lohrberg *et al*., 2002; Kubota *et al*., 1992; Shin and Ikohagi, 1999) and within a centrifugal impeller (Coutier-Delgosha *et al*., 2003) could be calculated using these inviscid flow models. Experimental observations have revealed that the cavitation appearance relates closely to the viscous phenomena of the liquid-phase, such as the boundary layer and the vortex motion. Recently, viscous flow models, which regard the cavitating flow as the bubbly flow containing spherical

Corresponding Author: Sandor I. Bernad, Romanian Academy-Timisoara Branch, Centre for Fundamental and Advanced Technical Research Bd. Mihai Viteazul 24, RO-300223, Timisoara, Romania

bubbles, were introduced to provide highly accurate calculations. In the viscous flow models, the Navier-Stokes equation including cavitation bubble is solved in conjunction with Rayleigh's equation governing the change in the bubble radius. Kubota *et al*., (1992) analyzed the flows around a hydrofoil by the Finite Diference method and (Bunnell and Heister, 2000) calculated the flow in a fuel injection pump for diesel engines by the control volume method. The predominating regions of high volumetric fraction of bubbles obtained by these methods agree well with the cavitation regions observed experimentally.

To account for the cavitation dynamics in a more flexible manner, recently, a transport equation model has been developed. In this approach volume or mass fraction of liquid (and vapor) phase is convected. Singhal *et al*. (1997), Merkle *et al*. (1998) and Kunz *et al*. (1999) have employed similar models based on this concept with diferences in the source terms. Merkle *et al*. (1998) and Kunz *et al*. (1999) have employed the artificial compressibility method. Kunz *et al*. (1999) have adopted a non-conservative form of the continuity equation and applied the model to diferent geometries. Their solutions are in good agreement with experimental measurements of pressure distributions.

The present study addresses the computational analysis of sheet hydrofoil cavitation. Other types of cavitation that occur with sheet cavitation include cloud and bubble cavitation. Sheet cavitation is very common on hydraulic machinery and the present study was motivated by studying the literature concerning the experimental observations and theoretical aspects. A sheet cavity is characterized by a distinct thin vapour bubble attached to the blade surface. Over the years several models have been developed that describe finite cavities. These are characterized by the manner in which the cavity is terminated.

Two-phase cavitating flow models based on homogeneous mixture approach, with a transport equation for the vapor volume fraction have been included in expert commercial codes such as FLUENT (Fluent 6, 2006).

We first evaluate this model for the benchmark problem of a NACA 0009 isolated hydrofoil and compare the numerical results with experimental data available in (Dupont, 1991).

METHODOLOGY

Cavitating flow model: Cavitating flow are very sensitive to the formation and transport of vapour bubbles, the turbulent fluctuations of pressure and velocity and to the magnitude of non-condensible gases, which are dissolved or ingested in the operating liquid (Shin and Ikohagi, 1999; Senocak and Shyy, 2002).

Numerical simulation of two-phase cavitating flows is an ongoing research effort with the ambitious goal to compute the unsteady evolution for cavities grow and collapse. The CFD community has developed so far a set of mature techniques for simulating single-phase viscous flows and the past half century of accumulated experience may very well serve to shape the numerical cavitating flow research. Early studies rely on the potential flow theory (Popp, 1985). This approach is now able to correctly describe partially cavitating two-dimensional hydrofoils, including the re-entrant jet cavity closure model (Krishnaswamy, 2000). However, extension to 3D problems and other types of cavitating flows seems to be out of reach for the potential flow model.

Although basic cavitation theoretical studies deal with bubble (or bubble clouds) dynamics by solving for the vapour-liquid interface, most of the practical cavitating flows are approached using a homogeneous flow theory. The main idea is to consider a single variable density fluid, without explicit phase interfaces. This model has emerged after carefully examining available experimental investigations, as well as by evaluating the computational costs involved in cavitating flows modelling. A review of cavitating flows numerical studies over the past decade can be found in Wang *et al*., (2001), where various Reynolds Averaged Navier-Stokes (RANS) solvers have been modified to account for the secondary phase (vapour and gas) dynamics.

The mixture model is used in the current study for the numerical simulation of cavitating flows with the FLUENT expert code (Fluent 6, 2006). In this model, the flow is assumed to be in thermal and dynamic equilibrium at the interface where the flow velocity is assumed to be continuous.

The *mixture* is a hypothetical fluid with variable density:

$$P_m = \alpha \rho_v + (1 - \alpha)\rho_l \quad (1)$$

ranging from liquid density for $\alpha = 0$ to vapour density ρ_v for $\alpha = 1$. The vapour volume fraction:

$$\alpha = \frac{Vol_{vapor}}{Vol_{liquid} + Vol_{vapor}} \quad (2)$$

is an additional unknown of the problem. The mixture will of course satisfy the continuity equation:

$$\frac{d\rho_m}{dt} + \rho_m \nabla . u_m = 0 \quad (3)$$

where, d/dt denotes the material derivative. Next, one has to consider a momentum equation for the mixture. A simple choice would be to neglect the viscous effects and

use the Euler equation. The system of equations can be then closed with a relationship density-pressure (equation of state). This approach can take advantage of a reach legacy of inviscid compressible solvers (Van der Heul *et al*., 2000). However, when considering a barotropic mixture, i.e. the density depends solely on the pressure, some physics is lost. This can be easily seen when writing the vorticity transport equation:

$$\frac{\partial \omega}{\partial t} + u.\nabla \omega = \omega.\nabla u + \frac{1}{\rho^2}\nabla p \times \nabla p + \text{viscous terms} \tag{4}$$

The second term in the right-hand-side, which accounts for the baroclinic vorticity generation, vanishes when $\rho = \rho(p)$. As a results, an important vorticity source is lost, especially in the cavity closure region (Senocak and Shyy, 2002).

Practical computations of industrial flows are using RANS equations with various turbulence modelling capabilities. This approach is embedded in most commercial codes currently available, e.g. FLUENT (Fluent 6, 2006). As a result, it seems natural to build a cavitating flow model on top of such computational infrastructure.

An alternative to the equation of state is to derive a transport equation for the vapour volume fraction. The continuity Eq. (3), together with Eq. (1), give the velocity divergence as:

$$\nabla \cdot u_m = -\frac{1}{\rho_m}\frac{d\rho_m}{dt} = \frac{\rho_l - \rho_v}{\rho_m}\frac{d\alpha}{dt}. \tag{5}$$

Using Eq. (5), the conservative form of the transport equation for α can be easily written:

$$\frac{\partial \alpha}{\partial t} + \nabla.\left(\alpha u_m\right) = \frac{1}{\rho_v}\left[\frac{\rho_v \rho_l}{\rho_m}\frac{d\alpha}{dt}\right] \tag{6}$$

Equation (6), can be also written for the liquid volume fraction, $1-\alpha$:

$$\frac{\partial (1-\alpha)}{\partial t} + \nabla.\left[(1-\alpha)u_m\right] = \frac{1}{\rho_l}\left[\frac{\rho_v \rho_l}{\rho_m}\frac{d\alpha}{dt}\right] \tag{7}$$

The factor in square brackets in the r.h.s. of Eq. (6) and (7) is the interphase mass flow rate per unit volume:

$$\dot{m} = \frac{\rho_v \rho_l}{\rho_m}\frac{d\alpha}{dt} \tag{8}$$

If we add term by term Eq. (6) and (7), we end up with an inhomogeneous continuity equation of the form

$$\nabla \cdot u_m = \dot{m}\left(\frac{1}{\rho_v} - \frac{1}{\rho_l}\right) \tag{9}$$

which is used in Eq. (6) to replace homogeneous Eq. (3).

Finally, the vapour volume fraction transport equation is written as:

$$\frac{\partial \alpha}{\partial t} + \nabla \cdot \left(\alpha u_m\right) = \frac{1}{\rho_v}\dot{m} \tag{10}$$

This is the equation for the additional variable α, to be solved together with the continuity and momentum equations.

Most of the efforts in cavitation modelling are focused on correctly evaluating $\dot{m}$. One approach has been proposed by Merkle *et al*. (1998), by modelling the phase transition process similar to the chemically reacting flows. This model was successfully employed by Kunz *et al*. (1999) in a variety of cavitating flows. However, the model constants are chosen somehow arbitrary and this choice ranges several orders of magnitude from one problem to another. Senocak and Shyy (2002) attempt a derivation of an empiricism-free cavitation model (Senocak and Shyy, 2002) in order to avoid the evaporation/condensation parameters introduced by Merkle.

A different approach is proposed by Schnerr and Sauer (2001), who consider the vapour-liquid mixture as containing a large number of spherical bubbles. As a result, the vapour volume fraction can be written as:

$$\alpha = \frac{n_b \frac{4}{3}\pi R^3}{1 + n_b \frac{4}{3}\pi R^3} \tag{11}$$

where, the number of bubbles per volume of liquid, n_b, is a parameter of the model.
From Eq. (11) we can easily get:

$$\frac{d\alpha}{dt} = \alpha(1-\alpha)\frac{3\dot{R}}{R} \tag{12}$$

where, $\dot{R}$ is the bubble vapour-liquid interface velocity. A simplified Rayleigh equation can be used to compute:

$$\dot{R} \equiv \frac{dR}{dt} = \text{sgn}\left(p_v - p\right)\sqrt{\frac{2}{3}\frac{\left|p_v - p\right|}{\rho_l}} \tag{13}$$

Of course the bubble grows if the mixture pressure is less than the vaporization pressure, $p < p_v$ and collapses

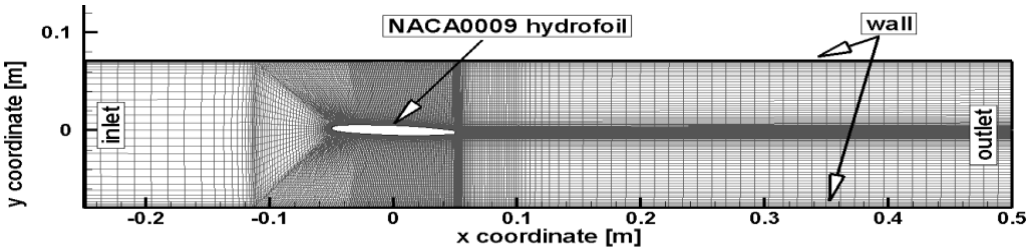

Fig. 1: Computational domain and boundary conditions for NACA 0009 hydrofoil

when $p > p_v$. The bubble collapse, as modelled by the Rayleigh second order differential equation, is much more rapid than the bubble growth. However, the above model seems to make no such difference between grow and collapse.

The present study employs the mixture model, as implemented in the FLUENT commercial code, with the cavitation model described by Eq. (8), (12) and (13).

Physically, the cavitation process is governed by thermodynamics and kinetics of the phase change process. The liquid-vapor conversion associated with the cavitation process is modeled through two terms, which represents, respectively, condensation and evaporation. The particular form of these phase transformation rates forms the basis of the cavitation model.

Numerical approach: To simulate the cavitating flow the numerical code FLUENT (Fluent 6, 2006) was used. The code uses a control-volume-based technique to convert the governing equations in algebraic equations that can be solved numerically. Being the governing equations non-linear (and coupled), several iterations of the solution loop must be performed before a converged solution is obtained. The flow solution procedure is the SIMPLE routine (Fluent 6, 2006). This solution method is designed for incompressible flows, thus being implicit. The full Navier-Stokes equations are solved. The flow was assumed to be steady and isothermal. In these calculations turbulence effects were considered using turbulence models, as the k-ϵ RNG models, with the modification of the turbulent viscosity for multiphase flow. To model the flow close to the wall, standard wall-function approach was used, then the enhanced wall functions approach has been used to model the near-wall region (i.e., laminar sublayer, buffer region and fully-turbulent outer region). For this model, the used numerical scheme of the flow equations was the segregated implicit solver. For the model discretization, the SIMPLE scheme was employed for pressure-velocity coupling, second-order upwind for the momentum equations and first-order up-wind for other transport equations (e.g., vapor transport and turbulence modeling equations). Computational domain is discretized using the GAMBIT preprocessor (Fluent 6, 2006). The flow close to the body surface is of particular importance in the current study, the mesh structure in the computational domain deliberately reflects this concern by heavily clustering the mesh close to the solid surface of the body so that the boundary layer mesh is used encloses the body surface.

Cavitating flow of a NACA 0009 hydrofoil: In this section we examine the fully-wetted flow and the partially cavitating flow for two-dimensional hydrofoils. The main reason for focusing on two-dimensional flow is that particular attention will be given to the method of simulating the flow at the end of the cavity which is a highly turbulent zone characterized by two-phase flow, unsteadiness and instabilities. Thus the rationale is to formulate an accurate model to simulate the two-dimensional flow prior to extending to three dimensions. Most cavity closure models have been formulated to comply with the theoretical analysis of the cavitating flow problem while at the same time attempting to model the physical reality.

The first case we shall present is that of a NACA 0009 hydrofoil at 2.5º angle of attack and a cavitation number equal to 0.81, investigated experimentally in Dupont (1991). The computational domain is consistent with the experimental setup presented by Dupont (1991). A structured quadrilateral mesh is used for computational domain discretization. Most of the cells are located around the foil and a contraction of the grid is applied in its upstream part, to obtain an especially fine discretization of the areas where cavitation is expected, Fig. 1.

Standard boundary conditions for incompressible flow are applied: the velocity is imposed at the inlet (V_{ref} = 20 m/s in the present case) and the pressure is fixed at the domain outlet. Then, the pressure is lowered slowly at each new time-step, down to the value corresponding to the desired cavitation number σ defined as $(P_{downstream}-P_{vap})/(\rho_{ref}V^2_{ref}/2)$. Vapor appears during the pressure decrease. The cavitation number is then kept constant throughout the computation.

The presence of a boundary layer will modify the main flow streamlines and subsequently the pressure

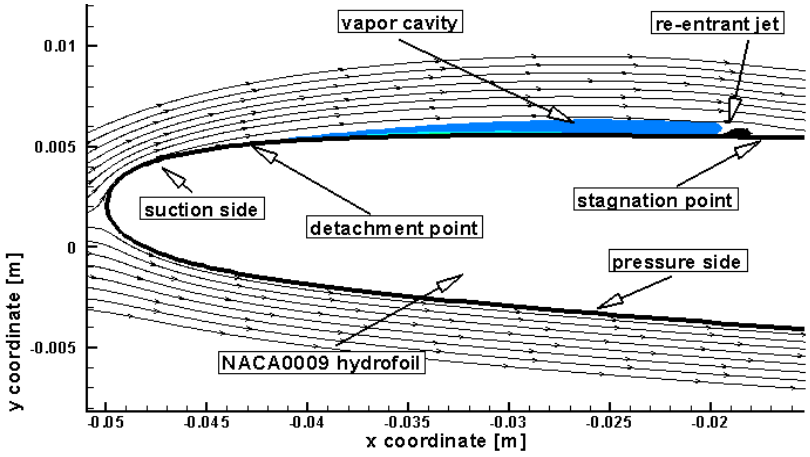

Fig. 2: Computed total volume franctions distributions and selected streamlines for NACA 0009 hydrofoil at cavitation number = 0.81

distribution along the guiding surface. It is important however to distinguish between a cavitation pocket which forms when the liquid detaches itself from the guiding surface, leaving a liquid-free zone and a separation pocket which forms when the boundary layer separates, leaving a liquid-filled zone. In nearly all cases, the initial point of separation will occur downstream from the point of minimum pressure as the flow up to this point is accelerating. However, cavitation is caused due to the reaching of a particular absolute pressure at any point in the flow. In general, this absolute pressure will be reached at or very close to the guiding surface. Thus at inception, cavitation will occur close to the point of minimum pressure on the surface.

Cavitation occurs as a result of the flow acceleration over the body surface resulting in regions with pressures lower than the vapor pressure. Then the water transform to vapor in these regions, thereby forming vapor-filled cavities. These cavities collapse when the local pressure becomes larger than vapor pressure, with a reentrant water jet and the flow generally becomes unsteady. Thus an irregular cyclic process of bubble formation and growth occurs, followed by the filling and finally breaking off of the bubble. Due to cavitation, large density and viscosity gradients arise at the interfaces between nearly incompressible fluids.

Within the cavity there are regions practically filled with gas (the first half) and regions with a gas-liquid mixture corresponding to the re-entrant jet dispersion and vaporisation, Fig. 2.

Figure 2 demonstrates the predictive capability of the model at cavitation numbers of 0.81 trough comparison with experimental data (Dupount, 1991).

The present numerical algorithm performs well for both cavitating and noncavitating conditions (Fig. 3). The

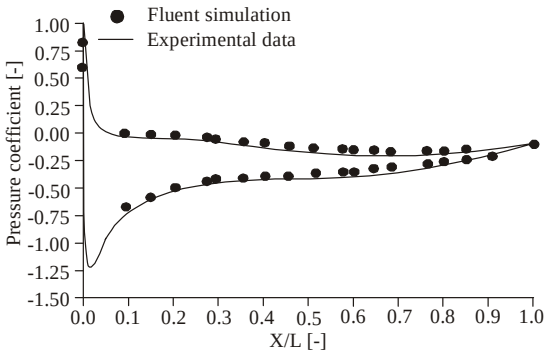

Fig. 3: Pressure coefficient distribution for NACA 0009 hydrofoil at no-cavitating condition, experimental data of Dupont (1991)

corresponding cavity profiles, streamlines and computed density ratios are also presented in Fig. 2 and 4.

The present simulation considers a steady flow, corresponding to a stable attached cavitation. However, when the re-entrant jet crosses the cavity boundary a large part of the cavity detaches and is transported downstream, while the remaining part starts growing again.

Visualisations of the velocity field show the development of a re-entrant jet along the hydrofoil, which is in agreement with the classical theory explaining the periodic shedding of vapour structures downstream from a cavity (Kubota *et al*., 1992; Kunz *et al*., 1999; Krishnaswamy, 2000). The qualitative analysis of the re-entrant jet formation is shown in Fig. 4.

The cavity closure is the region where the external flow re-attaches to the wall. The flow which originally moves along the cavity has locally the structure of a jet pinging obliquely upon the wall. The falling stream

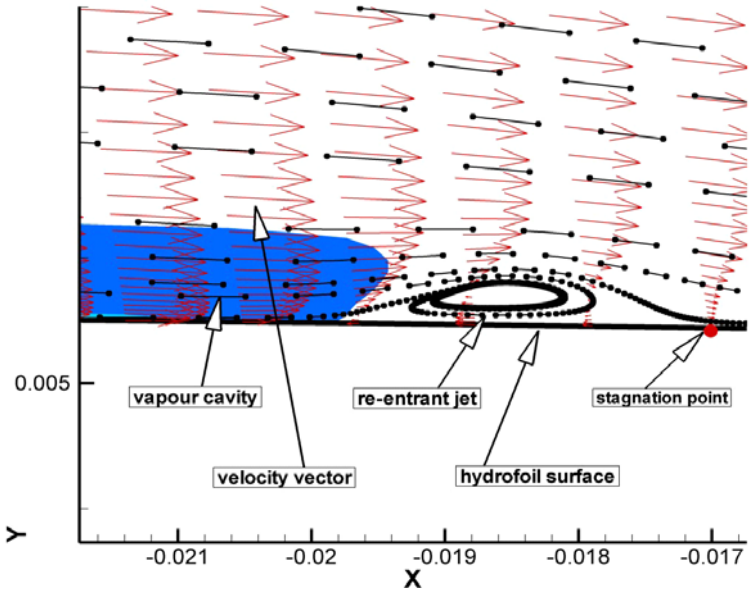

Fig. 4: Velocity vector field on the cavity end-zone showing the re-entrant jet formation under cavitating condition for NACA 0009 hydrofoil at cavitation number = 0.81

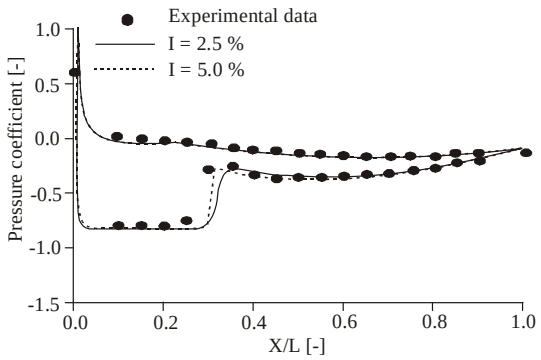

Fig. 5: Pressure coefficient distribution of the different turbulence intensity for NACA 0009 hydrofoil at no-cavitating condition (a) and (b) cavitation number = 0.81, experimental data of (Dupont, 1991)

divides into two parts flowing parallel to the wall. One is the re-entrant jet which moves upstream towards the cavity detachment. The other one makes the flow re-attach to the wall.

The gas void fraction contours at the two cavitation numbers are shown in Fig. 5. The simulation results indicate the cavity generated on this foil under cavitation number of 0.81 is of stable sheet cavity type.

For the cavitation number of 0.81, the cavity extends up to 30% of chord (Fig. 2). As the cavitation number increases the gas bubble region decreases in length and comes closer to the surface.

Figure 3 and 5 shows the comparison of numerical results with experimental data for both non-cavitating and cavitating flows over an isolated NACA 0009 hydrofoil at 2.5º angle of attack. An excellent agreement is obtained between simulation and experiment. Moreover, for cavitating flow we have investigated the effect of turbulence intensity on pressure distribution near the cavity closure. One can see that higher turbulence intensity tends to a sharper cavity closure (dashed line). Although the incoming turbulence intensity is one order of magnitude smaller in the cavitation tunnel, the turbulence intensity levels considered in the present investigation try to account for the flow induced hydrofoil vibrations.

RESULTS AND DISCUSSION

Three-dimensional cavitating flow in Francis turbine runner: The cavitating flow model described and validated in the above sections is further used to investigated a complex three-dimensional flow in the GAMM Francis turbine runner (Avellan *et al*., 1990; Avellan *et al*., 1993). The liquid steady turbulent relative flow in a runner interblade channel is first computed using a mixing interface approach (Muntean *et al*., 2004).

The operating conditions are set to achieve a cavitation number $\sigma = 0.1$:

$$\sigma = \frac{p_{atm} - p_v - \rho_l g H_s}{\rho_l E} = 0.1$$

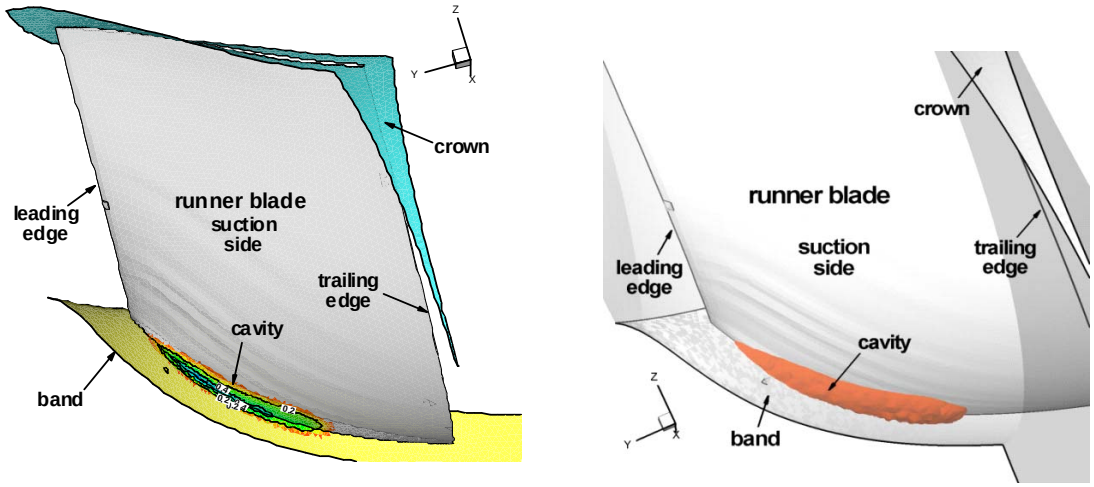

(a) (b)

Fig. 6a: Vapour volume fraction distribution on the GAMM francis turbine runner; b) cavity shape at σ = 0.1, presented as an iso-surface of $\alpha = 0.5$

with $p_{atm} = 17000\ pa$, $p_v = 2300\ pa$, $H_s = 0.9m$, and E = $60.33\ J/kg$. Note that the atmospheric pressure above is practically achieved for the turbine model by adjusting the overall pressure level in the hydraulic test rig.

The pressure coefficient is defined for GAMM Francis turbine as:

$$c_p = \frac{p - p_{ref}}{p_l E_{ref}}$$

where, p_{ref} is the pressure measured at the wall in a reference section downstream the runner, corresponding to the draft tube inlet.

Figure 6a shows the region on the runner blade suction side corresponding to $\alpha > 0$. It can be seen that cavitation occurs on the runner blade at the junction with the runner b and, where pressure drops below the vaporization pressure.

In order to evaluate the 3D shape and extend of the cavity, we are presenting in Fig. 6b the iso-surface of $\alpha = 0.5$. Of course, this is only a qualitative assessment of the cavity boundary, as one may choose another iso-surface as the cavity boundary. Nevertheless, the position, shape and size of the cavity seems to be in good agreement with the cavitating flow visualisation in GAMM Francis turbine runner, Fig. 7.

Note that the flow visualisation shows a travelling-cloud cavitation, where distinct bubbles can still be observed, Although the mixture model used here does not account for individual bubbles, the fact that α does not exceed 0.6 inside the cavity shows that there are no parts of the cavity completely filled with vapour.

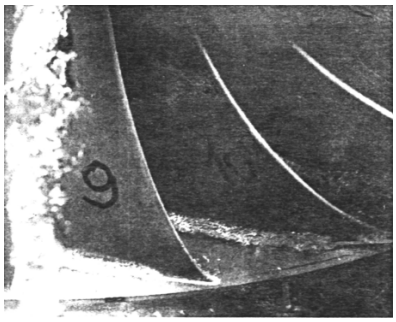

Fig. 7: Cavitating flow visualisation for the GAMM francis turbine, at $\sigma = 0.14$ (Avellan *et al*., 1990)

For $\sigma = 0.1$ the computed runner torque slightly increases from 374.3 N.m (liquid flow) to 375.6 N.m (cavitating flow). This is in good agreement with the turbine efficiency behaviour in the initial stage of the tolerated industrial cavitation regimes.

When the cavitation coefficient σ is further decreased, the cavity size (estimated as an iso-surface of vapour volume fraction $\alpha = 0.5$) increases. Figure 5 shows the cavity at $\sigma = 0.075$ and Fig. 8 at $\sigma = 0.05$. Moreover, Fig. 9 cleary shows the onset of the vortex rope on the crown.

The main advantage of directly computing the cavitating flows is that one can evaluate the influence of the cavity on the pressure distribution on the blade and further on the runner torque and turbine efficiency. Figure 10a shows the pressure distribution on the runner blade suction side, near the leading edge and at the blade-band

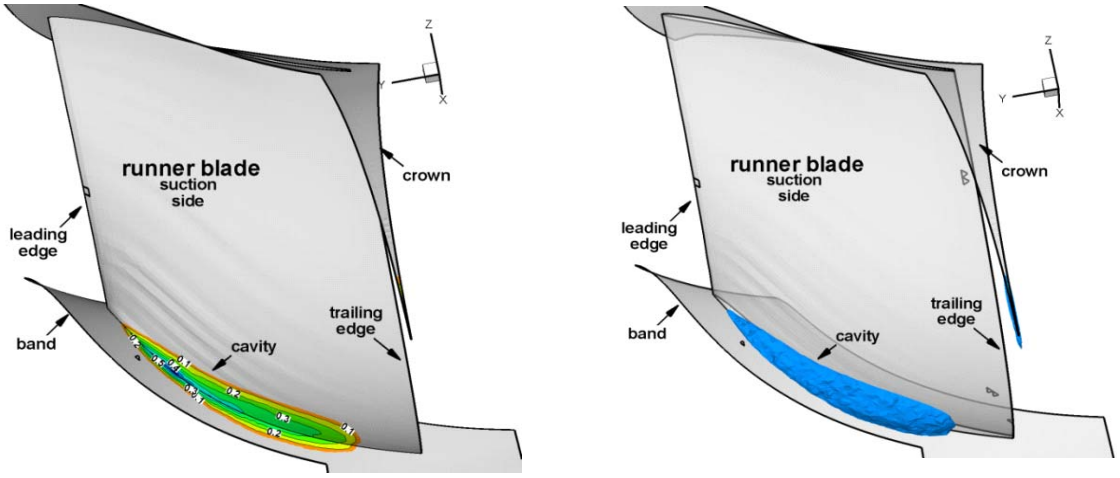

(a) (b)

Fig. 8: Vapour volume fraction distribution on the GAMM francis turbine runner. b) cavity shape at $\sigma = 0.075$; presented as an iso-surface of $\alpha = 0.5$

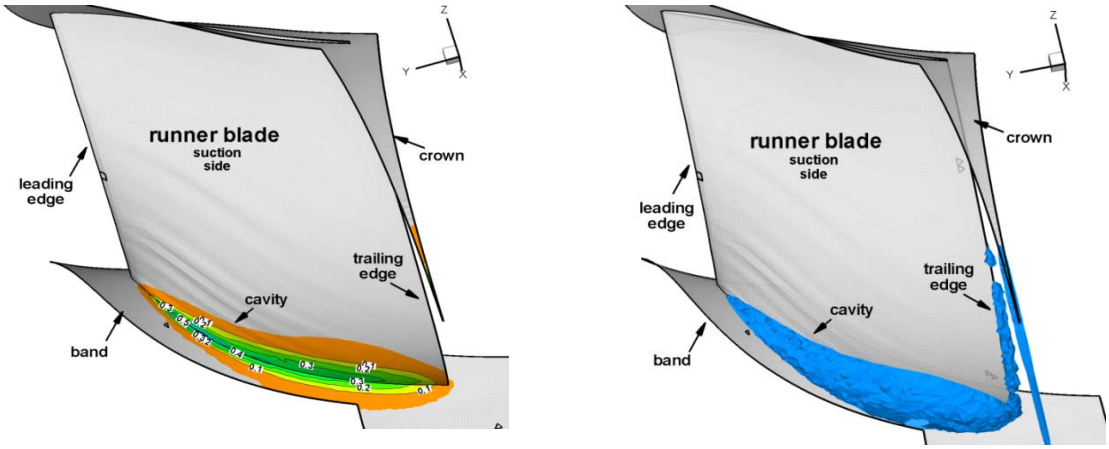

(a) (b)

Fig. 9: (a) Vapour volume fraction distribution on the GAMM Francis turbine runner; b) Cavity shape at $\sigma = 0.05$, presented as an iso-surface of $\alpha = 0.5$

junction, where no cavitation is presented (liquid flow). Several lines of constant c_p are shown.

The cavitation inception would occur theoretically if c_p drops below:

$$c_p = \frac{p - p_{ref}}{\rho_l E_{ref}} = \frac{2300 - 10275}{1000 \times 58.49} = -0.136$$

Note that the above reference pressure $p_{ref} = +10275Pa$ corresponds to a gauge reference pressure of $p_{ref}\big|_{gauge} = -6725Pa$. This value is correlated with a gauge pressure of – 0.1 *bar* at the center of runner outlet/draft tube inlet section.

The pressure of cavitation significantly changes locally the pressure distribution on the blade suction side. One can see from Fig. 10b that the lines of $c_p = -0.1$ and $c_p = -0.15$ significantly differ from those in Fig. 10a. The small distance between the two lines at intersection with blade-band junction in Fig. 10b corresponds to the relatively abrupt end of the cavity. There is no re-entrant jet in this case, but investigations are currently carried out at smaller cavitation numbers.

Measurements are available for c_p on the blade, on three selected sections. The section closest to the band is S15 (Avellan *et al*., 1990). Although S15 barely reaches the cavity, one can see from Fig. 11 that there are some small changes on the pressure induced by cavitation.

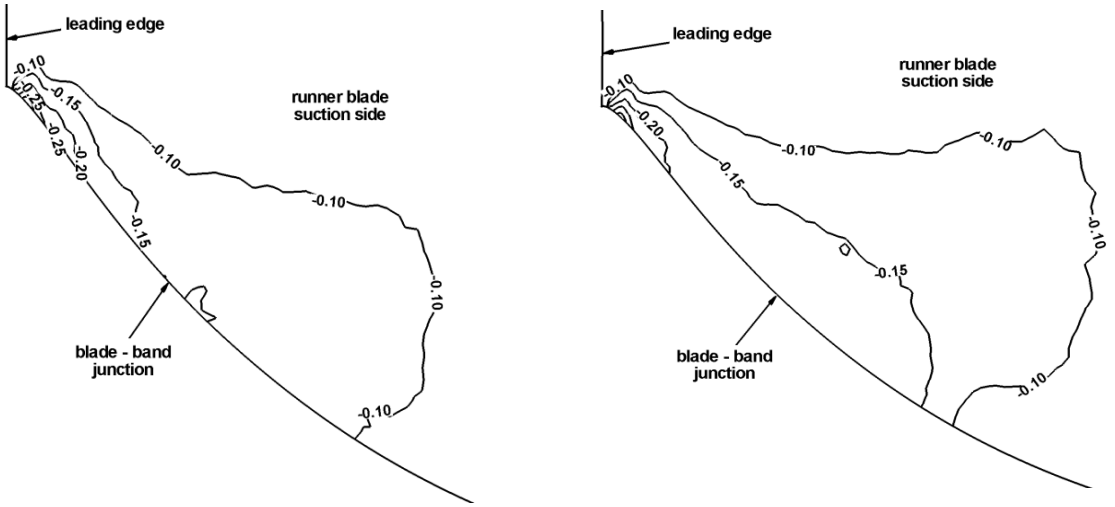

(a) (b)

Fig. 10: Detail of the pressure coefficient distribution on the runner blade suction side. a) flow without cavitation; b) cavitating flow with $\sigma = 0.1$

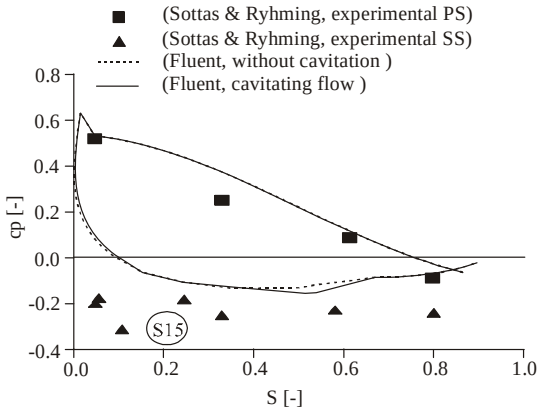

Fig. 11: Pressure coefficient distribution on the suction S15 of the runner blade (near the band)

The disagreement between the measured values on the suction side of S15 and numerical results has been debated in several studies so far, but it seems that no conclusion has emerged yet. For $\sigma = 0.1$ the computed runner torque slightly increases from 374.3 N.m (liquid flow) to 375.6 N.m (cavitating flow). This is in good agreement with the turbine efficiency behaviour in the initial stage of the tolerated industrial cavitation regimes.

CONCLUSION

The study presents a numerical investigation of cavitating flows using the mixture model implemented in the FLUENT commercial code. The inter-phase mass flow rate is modelled with a simplified Rayleigh equation applied to bubbles uniformly distributed in computing cells. The main advantage of this approach is that more accurate and reliable cavitation models can be introduced in the FLUENT code via the User Defined Functions.

The cavitation model is validated for the cavitating flow on a NACA0009 hydrofoil. The numerical results agree very well both qualitatively and quantitatively with the experiments.

The analysis of the pressure field without and with cavitation clearly demonstrates that for advanced cavitation stages one needs to compute a two-phase flow, otherwise the pressure field cannot be correctly estimated.

The results we have obtained so far correspond to a steady flow and therefore are valid for stable attached cavities. Further investigations will account for possible unsteadiness due to the cavity grow-detachment-collapse cycle.

As the authors proceed with this research, we are focusing on several areas including:

- Improved physical models for mass transfer and turbulence
- Extended application and validation for steady two-dimensional flows

Next, we investigate the 3D cavitating flow in the GAMM Francis turbine runner at the best efficiency point. The cavity shape and position is in good agreement with the flow visualisation. Moreover, we are able to quantify the local change in pressure distribution when

going from liquid flow to cavitating flow, as well as its influence on the runner torque value.

NOMENCLATURE

c_p [-]	Pressure coefficient
$\dot{m}$ [kg/(s.m^3)]	Inter-phase mass flow rate per unit volume
n_b [1/m^3]	Number of bubbles per unit volume of liquid
p [Pa]	Pressurerr
r [m]	Radius, radial coordinate
t[s]	Time
u [m/s]	Absolute velocity
x[m]	Axial coordinate
R [m]	Bubble radius
α [-]	Vapour volume fraction
ρ [kg/m^3]	density
$\omega = \nabla \times u$ [1/s]	Vorticityt
σ [-]	Cavitation number
Subscripts	
v	Vapour of vaporization
l	Liquid
∞	Points of large distance from the body
ref	Reference point
atm	Atmospheric pressure

ACKNOWLEDGMENT

This study has been supported by Romanian Academy annual program.

REFERENCES

Anton, I., 1984. Cavitation in Romanian. Romanian Academy Publishing House, Bucharest. Vol. 1, 1985 Vol. 2.

Avellan, F., P. Dupont, M. Farhat, B. Gindroz, P. Henry, M. Hussain, E. Parkinson and O. Santal, 1990. Flow survey and blade pressure measurements in a Francis turbine model. Proceedings of the XV IAHR Symposium, (Belgrade, Yugoslavia), 2(I5): 1-14.

Avellan, F., P. Dupont, M. Farhat, B. Gindroz, P. Henry and M. Hussain, 1993. Experimental Flow Study of the GAMM Turbine Model, 3D-Computation of Incompressible Internal Flows. NNFM 39, Edited by Sottas, G. and Ryhming I.L., Vieweg Verlag, Braunschweig, pp: 33-53.

Bunnell, R.A. and S.D. Heister, 2000. Three-dimensional unsteady simulation of cavitating flows in injector passages. J. Fluid Eng., 122: 791-797.

Coutier-Delgosha, O., J. Perrin, R. Fortes-Patella and J.L. Reboud, 2003. A numerical model to predict unsteady cavitating flow behaviour in inducer blade cascades. 15th International Symposium on Cavitation, Osaka, Japan.

Dupont, P., 1991. The dynamics of cavitation partial to the prediction of erosion in hydraulic turbomachines. PhD. Thesis, These No. 931, EPFL-Lausanne.

Krishnaswamy, P., 2000. Flow modelling for partially cavitating hydrofoils. Ph.D. Thesis, Technical University of Denmark.

FLUENT 6. 2006. User's Guide. Ansys-Fluent, Ansys Inc.

Kunz, R.F., D.A. Boger, T.S. Chyczewski, D.R. Stinebring and H.J. Gibeling, 1999. Multi-phase CFD analysis of natural and ventilated cavitation about submerged bodies. Proceeding of 3rd ASME/JSME Joint Fluid Engineering Conference, Paper FEDSM99-7364.

Kueny, J.L., 1993. Cavitation Modeling. Lecture Series: Spacecraft Propulsion. Von Karman Institute for Fluid Dynamics, January 25-29.

Kubota, A., H. Kato and H. Yamaguchi, 1992. A new modelling of cavitating flows: A numerical study of unsteady cavitation on a hydrofoil section. J. Fluid Mech., 240: 59-96.

Li, S.C., 2000. Cavitation of Hydraulic Machinery. Imperial College Press, UK.

Lohrberg, H., B. Stoffel, R. Fortes-Patella, O. Coutier-Delgosha and J.L. Reboud, 2002. Numerical and experimental investigations on the cavitating flow in a cascade of hydrofoils. Exp. Fluid., 33(4): 578-586.

Muntean, S., R.F. Susan-Resiga and I. Anton, 2004. Mixing Interface Algorithm for 3D Turbulent Flow Analysis of the GAMM Francis Turbine. In: Vad, J., T. Lajos and R. Schilling (Eds.), Modeling Fluid Flow. The State of the Art. Springer, Berlin, pp: 359-372.

Merkle, C.L., J.Z. Feng and P.E.O. Buelow, 1998. Computational modeling of the dynamics of sheet cavitation. 3rd International Symposium on Cavitation, pp: 307-311.

Popp, S., 1985. Mathematical Models in Cavity Theory. Technical Publishing House, Bucharest.

Shin, B.R. and T. Ikohagi, 1999. Numerical analysis of unsteady cavity flows around a hydrofoil. ASME-FEDSM 99-7215, (San Francisco).

Singhal, A.K., N. Vaidya and A.D. Leonard, 1997. Multi-Dimensional Simulation of Cavitating Flows Using a PDF Model for Phase Change. ASME FED Meeting, Vancouver, Canada, Paper No. FEDSM'97-32721997.

Schnerr, G.H. and J. Sauer, 2001. Physical and numerical modeling of unsteady cavitation dynamics. Proceeding of 4th International Conference on Multiphase Flow (New Orleans, U.S.A.).

Senocak, I. and W. Shyy, 2002. Evaluation of cavitation models for Navier-Stokes computations. Proceedings of the 2002 ASME Fluids Engineering Division Summer Meeting, Paper FEDSM2002-31011.

Van der Heul, D.R., C. Vuik and P. Wesseling, 2000. Efficient computation of flow with cavitation by compressible pressure correction. European Congress on Computational Methods in Applied Sciences and Engineering ECCOMAS-2000.

Wang, Y.C. and C.E. Brennen, 1994. Shock wave development in the collapse of a cloud of bubbles, ASME FED. Cavitat. Mult. Flow, 194: 15-19.

Wang, G., I. Senocak, W. Shyy, T. Ikohagi and S. Cao, 2001. Dynamics of attached turbulent cavitating flows. Prog. Aerospace Sci., 37: 551-581.